Agricultural and Forest Meteorology 192–193 (2014) 108–120

Contents lists available at ScienceDirect

Agricultural and Forest Meteorology

journal homepage: www.elsevier.com/locate/agrformet

Global comparison of light use efficiency models for simulating terrestrial vegetation gross primary production based on the LaThuile database

Wenping Yuan[a,b,*], Wenwen Cai[a], Jiangzhou Xia[a], Jiquan Chen[c,d], Shuguang Liu[e], Wenjie Dong[a,**], Lutz Merbold[f], Beverly Law[g], Altaf Arain[h], Jason Beringer[i], Christian Bernhofer[j], Andy Black[k], Peter D. Blanken[l], Alessandro Cescatti[m], Yang Chen[a], Louis Francois[n], Damiano Gianelle[o], Ivan A. Janssens[p], Martin Jung[q], Tomomichi Kato[r], Gerard Kiely[s], Dan Liu[a], Barbara Marcolla[o], Leonardo Montagnani[t,u], Antonio Raschi[v], Olivier Roupsard[w,x], Andrej Varlagin[y], Georg Wohlfahrt[z]

[a] State Key Laboratory of Earth Surface Processes and Resource Ecology, Beijing Normal University, Beijing 100875, China
[b] State Key Laboratory of Cryospheric Sciences, Cold and Arid Regions Environmental and Engineering Research Institute, The Chinese Academy of Sciences, Lanzhou, Gansu 730000, China
[c] International Center for Ecology, Meteorology and Environment, Nanjing University of Information Science and Technology, Nanjing 210044, China
[d] Department of Environmental Sciences, University of Toledo, Toledo, OH 43606, USA
[e] State Engineering Laboratory of Southern Forestry Applied Ecology and Technology, Central South University of Forestry and Technology, Changsha, Hunan 410004, China
[f] Department of Environmental Systems Science, ETH Zurich, Universitätsstrasse 2, 8092 Zurich, Switzerland
[g] College of Forestry, Oregon State University, Corvallis, OR 97331, USA
[h] McMaster Centre for Climate Change and School of Geography and Earth Sciences, McMaster University, Hamilton, Ontario, Canada
[i] School of Geography and Environmental Science, Monash University, Clayton, Victoria 3800, Australia
[j] Institute of Hydrology and Meteorology, Technische Universität Dresden, Dresden, Germany
[k] Faculty of Land and Food Systems, University of British Columbia, Vancouver, BC, Canada
[l] Department of Geography, University of Colorado at Boulder, Boulder, CO 80309-0260, USA
[m] European Commission, Joint Research Center, Institute for Environment and Sustainability, Ispra, Italy
[n] Institut d'Astrophysique et de Géophysique, Université de Liège, Bat. B5c, 17 Allée du Six Aout, B-4000 Liege, Belgium
[o] Sustainable Agro-ecosystems and Bioresources Department, IASMA Research and Innovation Centre, Fondazione Edmund Mach, 38010 San Michele all'Adige, TN, Italy
[p] University of Antwerpen, Department of Biology, Universiteitsplein 1, B-2610 Wilrijk, Belgium
[q] Max Planck Institute for Biogeochemistry, Jena, Germany
[r] Laboratoire des Sciences du CLimat et de l'Environnement, IPSL, CEA-CNRS-UVSQ Orme des Merisiers, F-91191 Gif sur Yvette, France
[s] Civil & Environmental Engineering Department, Environmental Research Institute, University College Cork, Ireland
[t] Forest Services, Autonomous Province of Bolzano, Via Brennero 6, 39100 Bolzano, Italy
[u] Faculty of Science and Technology, Free University of Bolzano, Piazza Università 5, 39100 Bolzano, Italy
[v] CNR – Institute of Biometeorology, 50145 Florence, Italy
[w] CIRAD, UMR Eco & Sols (Ecologie Fonctionnelle & Biogéochimie des Sols et des Agro-écosystèmes), 34060 Montpellier, France
[x] CATIE (Tropical Agricultural Centre for Research and Higher Education), 7170 Turrialba, Costa Rica
[y] A.N. Severtsov Institute of Ecology and Evolution, Russian Academy of Sciences, Moscow 119071, Russia
[z] Institute of Ecology, University of Innsbruck, Innsbruck 6020, Austria

ARTICLE INFO

Article history:
Received 30 June 2013
Received in revised form 22 February 2014
Accepted 9 March 2014
Available online 30 March 2014

Keywords:
Gross primary production
Light use efficiency
Seven LUE models

ABSTRACT

Simulating gross primary productivity (GPP) of terrestrial ecosystems has been a major challenge in quantifying the global carbon cycle. Many different light use efficiency (LUE) models have been developed recently, but our understanding of the relative merits of different models remains limited. Using CO_2 flux measurements from multiple eddy covariance sites, we here compared and assessed major algorithms and performance of seven LUE models (CASA, CFix, CFlux, EC-LUE, MODIS, VPM and VPRM). Comparison between simulated GPP and estimated GPP from flux measurements showed that model performance differed substantially among ecosystem types. In general, most models performed better in capturing the temporal changes and magnitude of GPP in deciduous broadleaf forests and mixed forests than in

* Corresponding author at: State Key Laboratory of Earth Surface Processes and Resource Ecology, Beijing Normal University, Beijing 100875, China.
** Corresponding author.
E-mail addresses: yuanwpcn@126.com (W. Yuan), dongwj@bnu.edu.cn (W. Dong).

http://dx.doi.org/10.1016/j.agrformet.2014.03.007
0168-1923/

evergreen broadleaf forests and shrublands. Six of the seven LUE models significantly underestimated GPP during cloudy days because the impacts of diffuse radiation on light use efficiency were ignored in the models. CFlux and EC-LUE exhibited the lowest root mean square error among all models at 80% and 75% of the sites, respectively. Moreover, these two models showed better performance than others in simulating interannual variability of GPP. Two pairwise comparisons revealed that the seven models differed substantially in algorithms describing the environmental regulations, particularly water stress, on GPP. This analysis highlights the need to improve representation of the impacts of diffuse radiation and water stress in the LUE models.

1. Introduction

Terrestrial gross primary productivity (GPP), about 20 times greater than the amount of carbon originating from anthropogenic source, is the largest component flux of the global carbon cycles (Canadell et al., 2007). Terrestrial GPP also provides important societal services through provision of food, fiber and energy. Regular monitoring of terrestrial GPP is therefore required to understand and assess dynamics in the global carbon cycle, forecast future climate, and ensure long term security of the services provided by terrestrial ecosystems (Bunn and Goetz, 2006; Schimel, 2007).

Numerous ecosystem models have been developed and widely used for quantifying the spatial-temporal variations in GPP. However, there exist substantial disagreement in the estimated magnitude and spatial distribution of GPP at regional and global scales using different ecosystem models. Previous comparison of 16 dynamic global vegetation models indicated that the lowest estimate of global net primary production (NPP) (39.9 Pg C yr^{-1}) was ~50% smaller than the maximum estimate (80.5 Pg C yr^{-1}) (Cramer et al., 1999). A recent study, comparing 17 models against observations from 36 North American flux towers, showed that none of the models consistently reproduced the interannual variability of GPP estimated from eddy covariance measurements within the measurement uncertainty (Keenan et al., 2012), and these models had very poor skill at the magnitude and temporal variations of GPP (Raczka et al., 2013).

In general, light use efficiency (LUE) models are not designed to predict future GPP because of the direct use of satellite data that are only available historically. However, LUE models may have the largest potential to adequately address the spatial and temporal dynamics of GPP because they take advantage of extensive satellite observations. Independently or as a part of integrated ecosystem models, the LUE approach has been used to estimate GPP and NPP at various spatial and temporal scales (Potter et al., 1993; Prince and Goward, 1995; Landsberg and Waring, 1997; Law et al., 2000; Coops et al., 2005). Some studies have evaluated LUE models at regional and global scales in major ecosystem types (Potter et al., 1993; Turner et al., 2006; Huntzinger et al., 2012; Yuan et al., 2012; Raczka et al., 2013; Cai et al., 2014).

LUE models are often developed based on particular assumptions with the processes controlling vegetation production formulated in different ways and diverse complexity. Each LUE model is a combination of equations describing environmental regulations of GPP (Beer et al., 2010). Recent studies have shown large model variations among different LUE models. For example, GPP estimates of North America from several satellite-based models varied considerably from 12.2 and 18.7 Pg C yr^{-1} (Huntzinger et al., 2012). Individual model validations are however not sufficient to identify the sources of the wide range of model differences. A rigorous comparison must be conducted in a standardized framework with consistent validation datasets and driving variables. In order to generate more robust estimates of vegetation production dynamics, it is necessary to compare estimates from a variety of LUE models and compare them against consistent and extensive measurements that are available (Running et al., 2004; Heinsch et al., 2006).

In this study, we evaluate how well seven satellite-based LUE models capture the spatial-temporal variations of GPP from the LaThuile FLUXNET dataset. The overarching goals of this study are to: (1) examine model performance across a network of flux sites, and (2) assess the importance of temperature and water stress in the seven LUE models.

2. Model and data

2.1. Light use efficiency model

The LUE model is built on two fundamental assumptions (Running et al., 2004): (1) ecosystem GPP is directly related to absorbed photosynthetically active radiation (*APAR*) through LUE, where LUE is defined as the amount of carbon produced per unit of *APAR*, and (2) LUE may be reduced below its theoretical potential value by environmental stresses such as low temperature or water shortage (Landsberg, 1986). The general form of the LUE model is:

$$GPP = PAR \times fPAR \times LUE_{\max} \times f(T_s, W_s, \ldots) \quad (1)$$

where *PAR* is the incident photosynthetically active radiation (MJ m^{-2}) per time period (e.g., day or month), *fPAR* is the fraction of *PAR* absorbed by the vegetation canopy (APAR), LUE_{max} is the potential LUE (g C m^{-2} MJ^{-1} APAR) without environment stress, f is a scalar varying from 0 to 1 that represents the reduction of potential *LUE* under limiting environmental conditions, T_s and W_s are temperature and water downward regulation scalars, and the multiplication of LUE_{max} and f is the actual LUE.

Seven LUE models were selected to conduct the global comparison of model performance, including CASA (Carnegie–Ames–Stanford Approach; Potter et al., 1993), CFix (Carbon Fix; Veroustraete et al., 2002), CFlux (Carbon Flux; Turner et al., 2006; King et al., 2011), EC-LUE (Eddy Covariance-Light Use Efficiency; Yuan et al., 2007a, 2010; Li et al., 2013), MODIS-GPP (Moderate Resolution Imaging Spectroradiometer; Running et al., 2004), VPM (Vegetation Production Model; Xiao et al., 2004a) and VPRM model (Vegetation Production and Respiration Model; Mahadevan et al., 2008). Detailed model description and model operation can be found from the Supplemental Online Material (SOM).

2.2. Data and methods

We used the LaThuile FLUXNET dataset (http://www.fluxdata.org) to evaluate model performance. In total, 157 eddy covariance (EC) towers were included in this study covering six major terrestrial biomes: evergreen broadleaf forest (EBF, 14 sites), deciduous broadleaf forest (DBF, 25 sites), mixed forest (MIF, 9 sites), evergreen needleleaf forest (ENF, 62 sites), shrubland (SHR, 5 sites) and grassland (GRS, 42 sites) (Table S1 and Fig. S1). Detailed information on data processing and site

information (i.e. vegetation, climate and soils) are available at the LaThuile FLUXNET web site. Briefly, the gap-filling technique used was the method described in Reichstein et al. (2005) that exploits both the co-variation of fluxes with meteorological variables and the temporal autocorrelation of fluxes. The partitioning between GPP and terrestrial ecosystem respiration has been done according to the method proposed in Reichstein et al. (2005). Eddy covariance systems directly measure net ecosystem exchange (NEE) rather than GPP. In order to estimate GPP, it is necessary to estimate daytime respiration (Rd):

$$\mathrm{GPP} = \mathrm{R}_d - \mathrm{NEE}_d \quad (2)$$

where $\mathrm{NEE_d}$ is daytime NEE. Daytime ecosystem respiration $\mathrm{R_d}$ is usually estimated by using daytime temperature and an equation describing the temperature dependence of respiration, which is subsequently developed from nighttime NEE measurements. Nighttime NEE represents nighttime respiration because plants do not photosynthesize at night. The following model (Lloyd and Taylor, 1994) was used to describe the effects of temperature on night-time NEE:

$$\mathrm{NEE_{night}} = \mathrm{R_{ref}} \times e^{E_0 \times (1/T_{ref} - T_0 \times 1/T - T_0)} \quad (3)$$

where $\mathrm{NEE_{night}}$ is night-time ecosystem respiration, T is average air temperature at night time. The regression parameter T_0 is kept constant at −46.02 °C as in Lloyd and Taylor (1994), and the reference temperature (T_{ref}) is set to 10 °C as in the original model. The parameters E_0 (activation energy) and R_{ref} (reference ecosystem respiration) were determined using nonlinear optimization. Eq. (3) and daytime temperature were subsequently used to estimate daytime respiration (R_{d}).

We examined model performance using calibrated parameter values at all sites. Fifty percent of the sites were selected to calibrate model parameters for each vegetation type, and the remaining 50% of the sites were used to validate the models. This parameterization process was repeated until all possible combinations of 50% sites were achieved for each vegetation type. The nonlinear regression procedure (Proc NLIN) in the Statistical Analysis System (SAS, SAS Institute Inc., Cary, NC, USA) was applied to optimize the model parameters using daily estimated GPP based on EC measurements. Mean calibrated parameter values, (Table 1), were used to simulate GPP at all sites.

In this study, we examined model performance in three ways: model's ability in simulating daily GPP variations at all sites, model performance in capturing spatial variability of GPP, and model representation of the interannual variability of GPP. Two criteria were imposed during data screening. First, if >20% of the daily data for a given year were missing, all data from that year were indicated as missing and discarded. Second, a single site had to have a minimum of five years of GPP observations and simulations to be included in the evaluation of interannual variability. Based on these criteria, 51 sites consisting of 307 years of observations were included for examining the model performance on interannual variability of GPP (Table S1). We conducted the correlation analysis of annual mean GPP simulations and EC-GPP estimates at each site, and examined their correlations for all 51 sites. Moreover, standard deviation of annual GPP was used to indicate the magnitude of interannual variability. We analyzed the correlation of standard deviations of simulated GPP and those of the EC-GPP estimates to examine model's ability on capturing the magnitude of variation.

In order to examine the performance of models under different cloudy cover conditions, a daily cloudiness index (CL), i.e. the ratio of daily PAR to potential PAR, was used to indicate cloud cover fraction. Days with $CL < 0.3$ were considered to be mostly cloudy, 0.3–0.6 as partly cloudy, and >0.6 as clear. Similarly, water stress, calculated from water stress scalars of the seven models using the following equations, was separated into three levels (i.e. high, normal and low) to facilitate a consistent comparison of simulated water stress among the seven models:

$$\begin{cases} \text{High water stress}, & W_s < W_{s\min} + \dfrac{W_{s\max} - W_{s\min}}{3} \\ \text{Normal water stress}, & \left(W_{s\max} + \dfrac{W_{S\max} - W_{s\min}}{3}\right) \le W_s \le \left(W_{s\min} + \dfrac{2 \times (W_{s\max} - W_{s\min})}{3}\right) \\ \text{Low water stress}, & W_s > W_{s\min} + \dfrac{2 \times (W_{s\max} - W_{s\min})}{3} \end{cases} \quad (4)$$

where W_{smin} and W_{smax} are the minimum and maximum values of W_{s} through the entire study period at each site.

Two pairwise comparisons were conducted on model components for investigating the differences of model structure. First, we identified the impacts of fPAR on GPP simulations by comparing two correlations:

(a) Correlation of simulated GPP among seven models;
(b) Correlation of simulated potential GPP ($PGPP$) assuming no environmental stress (i.e. $PAR \times fPAR \times LUE_{max}$);

Second, we diagnosed the primary environmental variables by performing pairwise comparison of:

(a) Correlation of temperature limited GPP (GPP_{tem}) (i.e. $PAR \times fPAR \times LUE_{max} \times f(T_s)$);
(b) Correlation of water limited GPP (GPP_{water}) (i.e. $PAR \times fPAR \times LUE_{max} \times f(W_s)$).

2.3. Statistical analysis

Three metrics were used to evaluate the performance of the models, including Correlation coefficient of determination (R^2), root mean square error (RMSE), and mean predictive error (BIAS, difference between mean observations and simulations).

3. Results

3.1. Comparison of model performance

The seven LUE models showed substantial differences in model performance for simulating daily GPP variations among ecosystem types (Fig. 1). For the shrublands and evergreen broadleaf forests, all models showed low performance with low R^2 and high RMSE. The best model performance was observed in deciduous broadleaf forests. For a given vegetation type, model performance differed. Across all ecosystem types, CFlux and EC-LUE showed the highest R^2 and lowest RMSE when compared to the remaining five models (Fig. 1). Moreover, the CFlux and EC-LUE showed better performance than other five models at shrublands, deciduous broadleaf forests, evergreen needleleaf forests and grasslands. The CFlux and EC-LUE had lower RMSE than the mean RMSE of the seven models at 76% and 75% sites, respectively, and higher R^2 than the mean R^2 at 80% and 75% sites, respectively (Fig. 2).

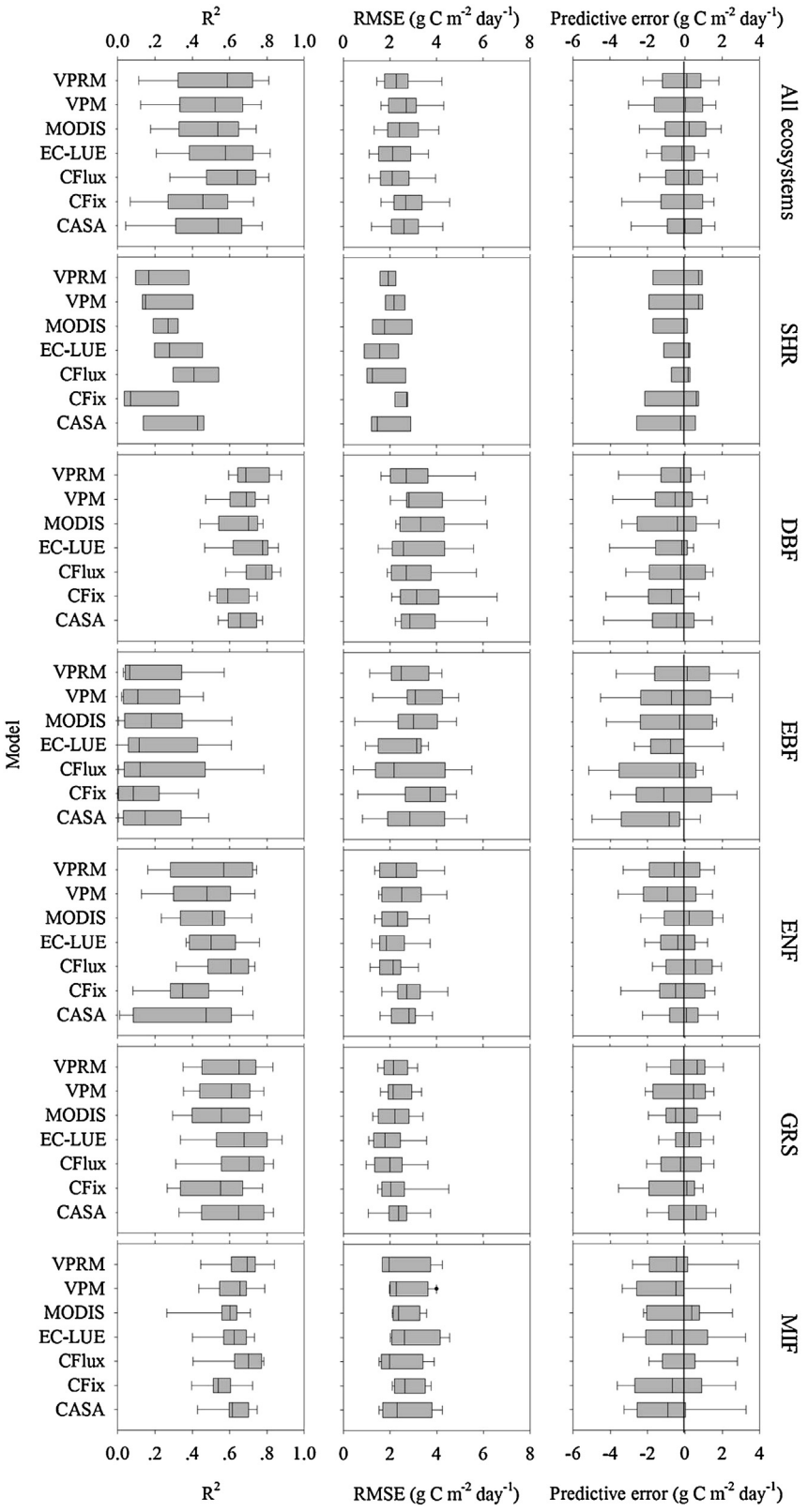

Fig. 1. Model performance of seven light use efficiency models for simulating daily GPP with calibrated parameters at various vegetation types. SHR: shrubland; DBF: deciduous broadleaf forest; EBF: evergreen broadleaf forest; ENF: evergreen needleleaf forest; GRS: grassland; MIF: mixed forest. Boxplots with median, upper and lower quartile, minimum and maximum values. Model validations were conducted at the daily scale.

Moreover, we investigated the performance of the seven models in reproducing site-averaged daily GPP. The EC-LUE model explained a larger portion ($R^2 = 0.55$) of the spatial GPP variation than other models (Fig. 3d). All models showed an overestimation of GPP in low GPP regions, and underestimation in high GPP regions (Fig. 3, S2). The predictive errors of the seven models were significantly correlated with the estimated GPP from EC measurements (Fig. 3, S2). However, it is apparent that the slopes of the EC-LUE

Table 1
Calibrated model parameter values for seven models.

Parameter	Vegetation type					
	SHR	DBF	EBF	ENF	GRS	MIF
CASA						
LUE_{max}	0.62 ± 0.20	1.22 ± 0.43	0.87 ± 0.15	0.85 ± 0.18	0.78 ± 0.17	1.04 ± 0.36
CFix						
LUE_{max}	1.89 ± 0.35	1.79 ± 0.27	1.92 ± 0.18	1.85 ± 0.35	1.94 ± 0.19	1.86 ± 0.33
LUE_{min}	0.55 ± 0.26	1.27 ± 0.07	1.33 ± 0.15	1.09 ± 0.06	1.14 ± 0.09	1.16 ± 0.13
CFlux						
LUE_{max}	1.12 ± 0.28	3.07 ± 0.25	3.02 ± 0.18	2.29 ± 0.12	2.53 ± 0.15	2.53 ± 0.25
LUE_{cs}	0.66 ± 0.05	1.17 ± 0.07	1.12 ± 0.10	0.95 ± 0.05	1.08 ± 0.08	1.05 ± 0.13
$TMIN_{min}$	−13.76 ± 6.54	−4.35 ± 2.13	−14.46 ± 4.35	−14.20 ± 2.40	−20.12 ± 7.06	−14.26 ± 4.17
$TMIN_{max}$	13.04 ± 8.79	13.08 ± 3.23	20.00 ± 0.00	8.25 ± 1.82	9.55 ± 5.87	13.79 ± 3.74
VPD_{min}	0.33 ± 0.34	0.11 ± 0.01	0.12 ± 0.07	0.11 ± 0.00	0.12 ± 0.01	0.12 ± 0.02
VPD_{max}	3.42 ± 0.58	2.99 ± 0.32	2.56 ± 0.32	2.79 ± 0.13	3.23 ± 0.47	2.44 ± 0.32
EC-LUE						
LUE_{max}	1.28 ± 0.40	1.71 ± 0.19	1.70 ± 0.11	1.85 ± 0.20	1.59 ± 0.41	1.72 ± 0.31
MODIS						
LUE_{max}	0.66 ± 0.28	1.77 ± 0.19	1.68 ± 0.10	1.36 ± 0.08	1.52 ± 0.16	1.64 ± 0.22
$TMIN_{min}$	−13.76 ± 6.54	−4.35 ± 2.13	−14.46 ± 4.35	−14.20 ± 2.40	−20.12 ± 7.06	−14.26 ± 4.17
$TMIN_{max}$	13.04 ± 8.79	13.08 ± 3.23	20.00 ± 0.00	8.25 ± 1.82	9.55 ± 5.87	13.79 ± 3.74
VPD_{min}	0.33 ± 0.34	0.11 ± 0.01	0.12 ± 0.07	0.11 ± 0.02	0.12 ± 0.01	0.12 ± 0.02
VPD_{max}	3.42 ± 0.58	2.99 ± 0.32	2.56 ± 0.32	2.79 ± 0.13	3.23 ± 0.47	2.44 ± 0.32
VPM						
LUE_{max}	1.25 ± 0.43	2.11 ± 0.11	2.17 ± 0.16	2.17 ± 0.10	1.92 ± 0.12	2.03 ± 0.24
VPRM						
LUE_{max}	4.42 ± 1.88	8.63 ± 1.14	10.88 ± 2.17	14.89 ± 2.10	7.87 ± 1.08	10.16 ± 3.04
PAR_0	4.47 ± 1.22	3.15 ± 0.44	2.37 ± 0.75	1.61 ± 0.24	3.07 ± 0.52	2.50 ± 0.81

SHR: shrubland; DBF: deciduous broadleaf forest; EBF: evergreen broadleaf forest; ENF: evergreen needleleaf forest; GRS: grassland; MIF: mixed forest. Mean optimized parameters with one standard deviation were shown in the table. Parameters were described at the Supplemental Online Material.

in the regression equation of predictive errors with estimated GPP from flux measurements were closer to zero, with lower R^2 (Fig. 3, S2).

All but the CFlux model significantly underestimated GPP during cloudy days (Fig. 4). The mean predictive errors of the CFlux model were 0.12 ± 1.74, 0.16 ± 1.59 and $0.17 \pm 1.30\,g\,C\,m^{-2}\,day^{-1}$ at clear, partly cloudy and mostly cloudy days, respectively, and the differences were not significantly different ($p = 0.05$) (Fig. 4c). One the other hand, the other six models showed significant performances between clear days and cloudy days. For example, the averaged predictive errors of the CASA model were about $-1.12 \pm 1.30\,g\,C\,m^{-2}\,day^{-1}$ at the mostly cloudy days and $0.15 \pm 1.91\,g\,C\,m^{-2}\,day^{-1}$ for clear days (Fig. 4a).

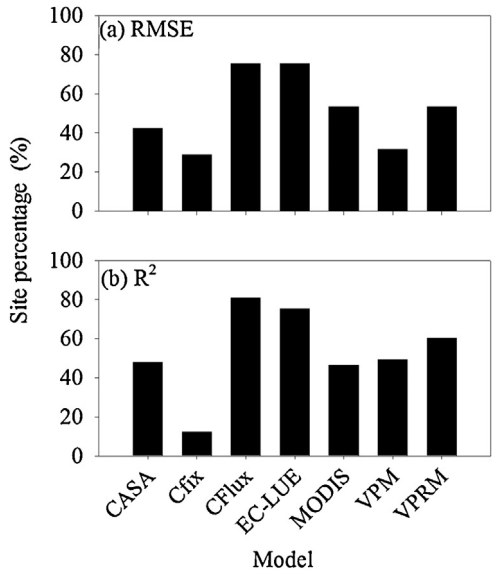

Fig. 2. Percentage of eddy covariance sites where (a) RMSE of individual model < RMSE of mean values of seven models and (b) R^2 of individual model > R^2 of mean values of seven models.

The ability to simulate interannual variability was investigated at 51 sites with more than five-year observations. Results indicated the seven LUE models performed poor in capturing the interannual variability of GPP. The mean values of correlation coefficient (R^2) of the simulated GPP and EC-GPP estimates ranged from 0.06 to 0.36 for all sites. The EC-LUE and CFlux models showed the highest R^2 of 0.36 and 0.30 (Fig. 5c and d). At most sites, the slopes of regression relationship deviated from 1, and averaged slopes ranged from 0.19 to 0.56. The EC-LUE and CFlux models had largest mean values of slope with 0.56 and 0.40, respectively (Fig. 5j and k). The correlation coefficient (R^2) of the standard deviations between simulated GPP and estimated GPP based on EC measurements through all sites ranged from 0.03 to 0.38, indicating a poor ability of the seven LUE models in identifying the magnitude of the interannual variability of GPP (Fig. 6). The EC-LUE showed the highest correlation coefficient of 0.38 (Fig. 6d).

3.2. Comparisons of model structure

The first pairwise comparison showed higher correlations of daily PGPP (i.e. $PAR \times fPAR \times LUE_{max}$) among the seven models compared with GPP simulations (Fig. 7). For example, the correlations of PGPP between the CASA model and the remaining six models ranged from 0.75 to 0.96. In contrast, correlations of GPP simulations ranged from 0.37 to 0.43 for the same comparison. Such a pairwise comparison of PGPP and GPP simulations can essentially indicate the contributions of fPAR and environment regulation scalars to the differences in GPP simulations. The results further suggest that the differences between models were due more to the response of the models to environmental stresses compared with the response of the models to fPAR.

The second pairwise comparison indicated that the model differences were predominantly driven by the way in which water stress was parameterized in the models compared to that of

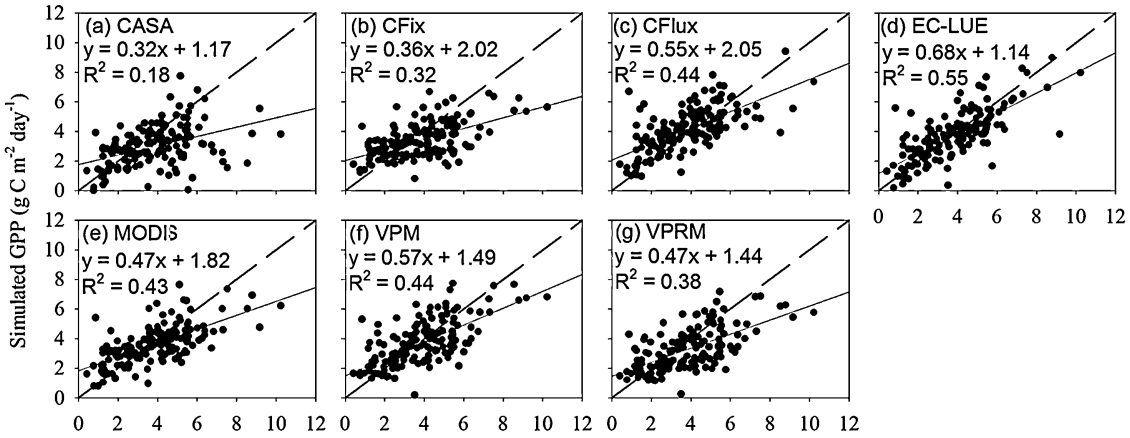

Fig. 3. Estimated GPP based on eddy covariance measurements vs. the simulated GPP over the 157 EC sites with calibrated parameters. The long dash lines are 1:1 line and the solid lines are linear regression line. The dots indicate the site-averaged GPP.

temperature stress (Fig. 8). On average, the correlation of GPP_{tem} between two models was 0.80 ± 0.08, while the mean value of correlations of GPP_{water} was 0.65 ± 0.12.

We compared the ability of the seven models to simulate water stress by separating water stress conditions of each model into three levels: high, normal and low water stresses (see method section). Our results showed >50% of the study time the seven models did not identify the same level of water stress (Table 2). For example, on average, 65% water stress levels were inconsistent between the MODIS and EC-LUE models (Table 2). Our results also presented a large fraction of inconsistency in identifying low and high water stress conditions. Among the seven models, on average, >15% days were incorrectly identified between high and low water stresses (Table 2). Significant differences of model performance were found among the seven LUE models across the three water stress conditions (i.e. high, normal and low) (Fig. 9). Other than the CFlux, VPRM and VPM, the remaining four models showed low R^2 at high water stress. For example, the CFix model explained $\sim 50 \pm 25\%$ of the variation in GPP estimated for wet conditions, but only explained $22 \pm 15\%$ of the variation in GPP during high water stress (Fig. 9). Finally, no consistent predictive errors were found under the different water stresses among the seven models. The CASA model tended to underestimate GPP while the CFix model showed overestimation of GPP in drought days (Fig. 9).

4. Discussion

4.1. Model performance

None of the model predictions in this study matched well with estimated GPP based on EC measurements for all vegetation types. On average, seven models explained 41–57% GPP variations over all study sites (Fig. 1). Two models (i.e. CFlux and EC-LUE) achieved a slightly better performance, with higher model accuracy than the average levels of seven models over all sites (Fig. 2). Moreover, we found statistically significant differences in model performance within vegetation types. All of the seven models showed poor performance for the shrublands and evergreen broadleaf forests, and good performance for deciduous broadleaf forests and mixed forests. This conclusion was supported by a recent model evaluation, based on 17 models against observations from 36 North American flux towers, which reveal the models perform the best for deciduous broadleaf sites, but not well for evergreen sites (Raczka et al., 2013). Few studies investigated the model performance difference at different vegetation types. In general, deciduous broadleaf forests demonstrate distinct seasonal dynamics of leaf phenology (leaf emergence, leaf senescence and leaf fall), and satellite data can accurately capture the phenology change. Moreover, dominating factors of vegetation production can be explicitly identified at different phenology periods (Yuan et al.,

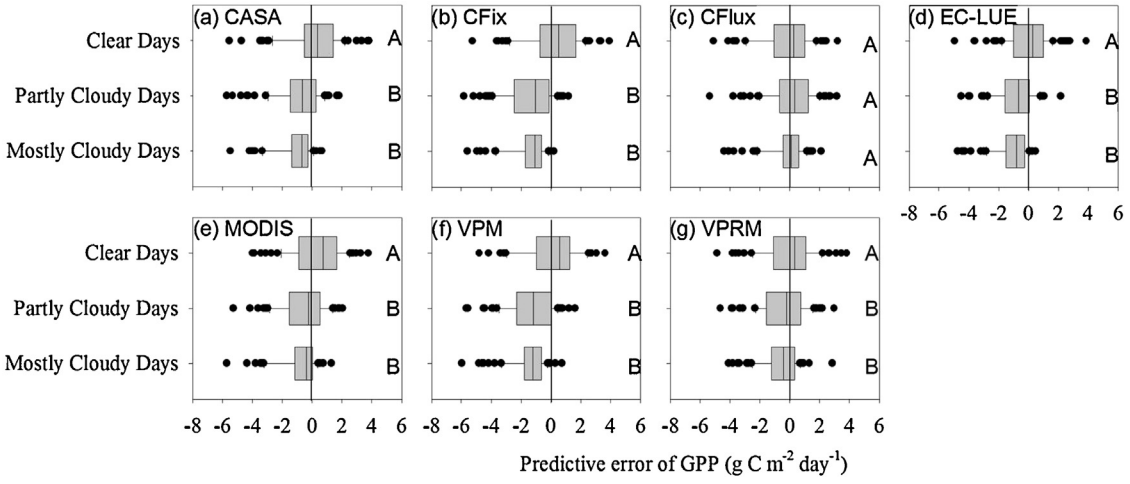

Fig. 4. Predictive error of GPP derived seven models at clear, partly cloudy and mostly cloudy days for seven models. Different letters within the figures indicate statistically significant differences ($p < 0.05$).

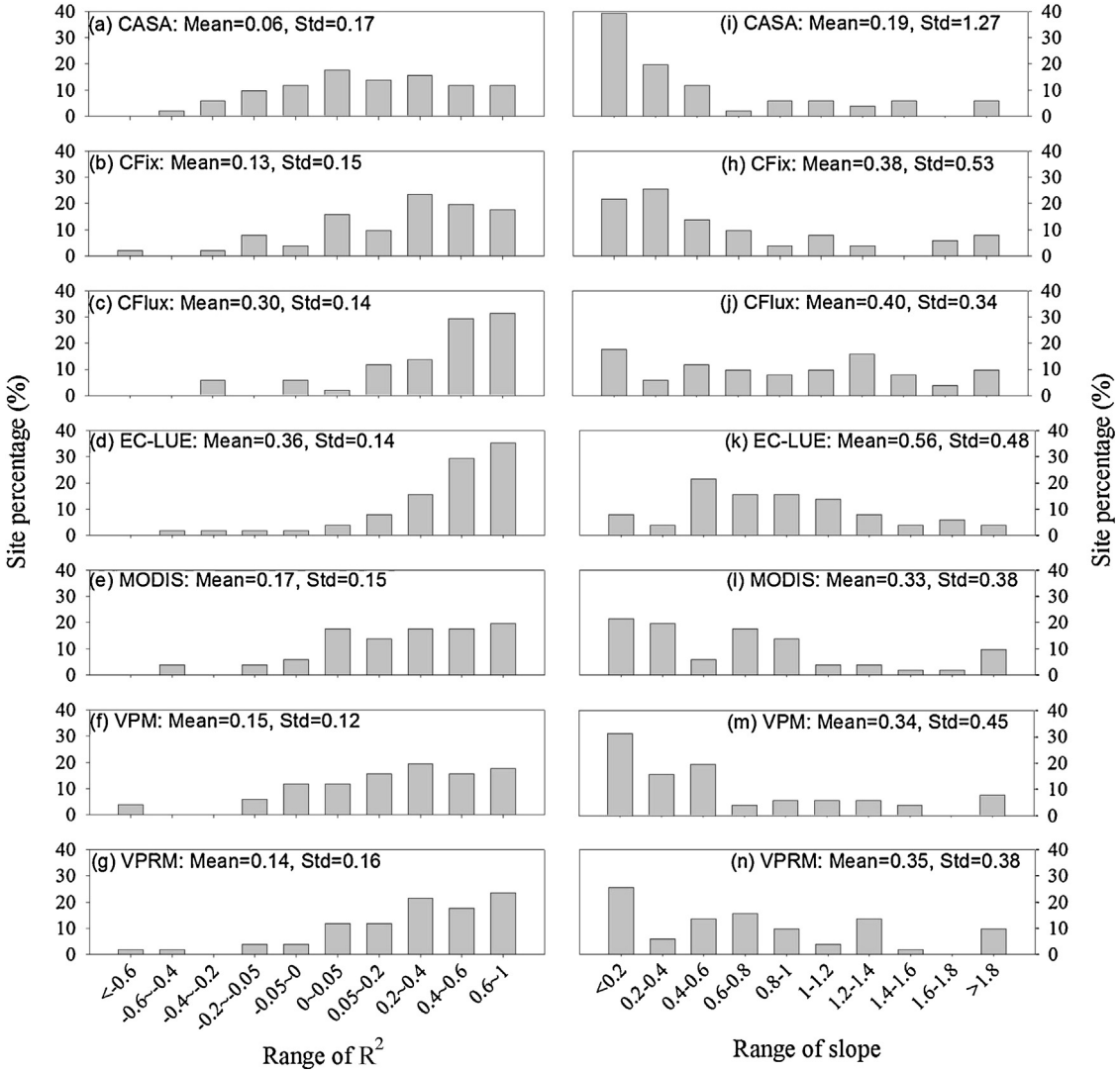

Fig. 5. Site percentage of correlation coefficients (R^2) and slopes of regression relationships between simulated and observed interannual variability of GPP. *Mean* and *Std* in the figures indicate the mean value and standard deviation of R^2 and slope at all 51 sites.

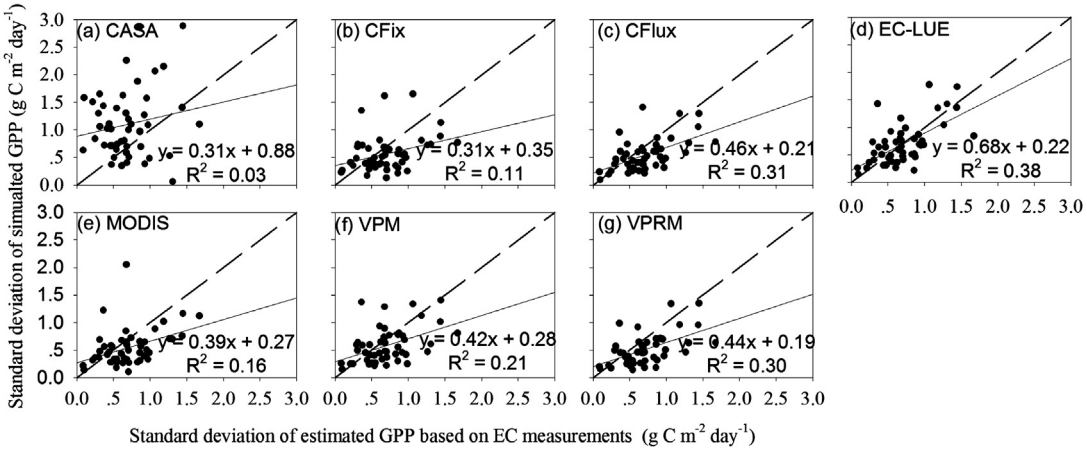

Fig. 6. Correlation between site-averaged standard deviations of simulated GPP and estimated GPP based on eddy covariance measurements. The long dash lines are 1:1 lines and the solid line are linear regression lines.

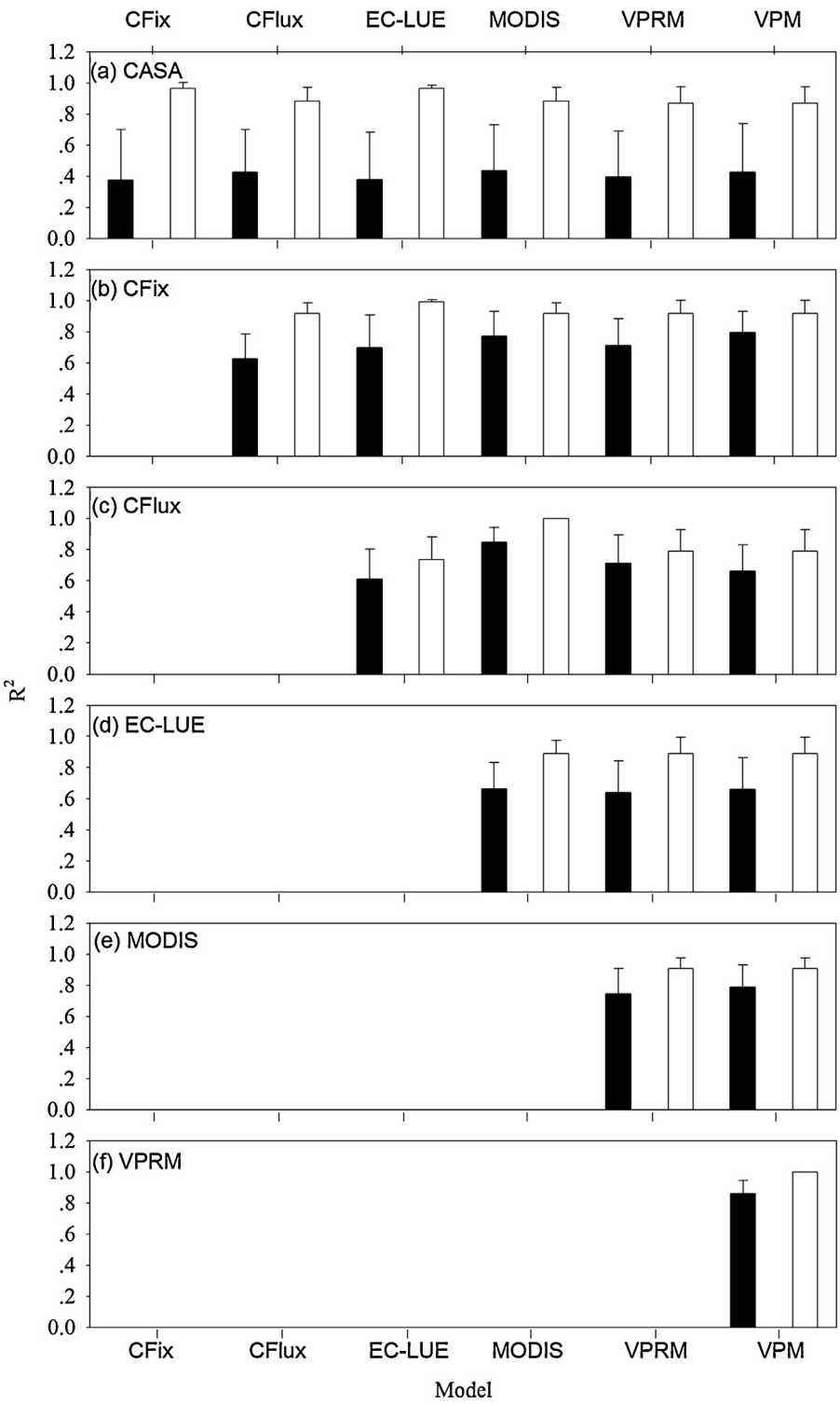

Fig. 7. Comparison of mean coefficient of determination (R^2) of GPP simulations (black bar) and potential GPP (PGPP, white bar) among seven LUE models.

2007), which is beneficial to LUE models. On the contrary, evergreen broadleaf forest reveals subtle changes in the seasonal leaf phenology, and various environment factors jointly determine plant photosynthesis, which increase the difficulty in modeling (Xiao et al., 2004a).

The results revealed the difficulty in modeling interannual variability of GPP, as the seven models only explained 6–36% interannual variability of GPP (Fig. 5). Previous studies have revealed a large uncertainty among LUE models. For example, a model comparison, which assessed the performance of 16 terrestrial biosphere models and 3 remote sensing products at 11 forested sites in North America, found that none of the models consistently reproduced the observed interannual variability (Keenan et al., 2012). Possible causes of the errors for modeling spatial and temporal variations of GPP include: (1) LUE models do not completely integrate the environmental regulations to vegetation production; (2) any errors in

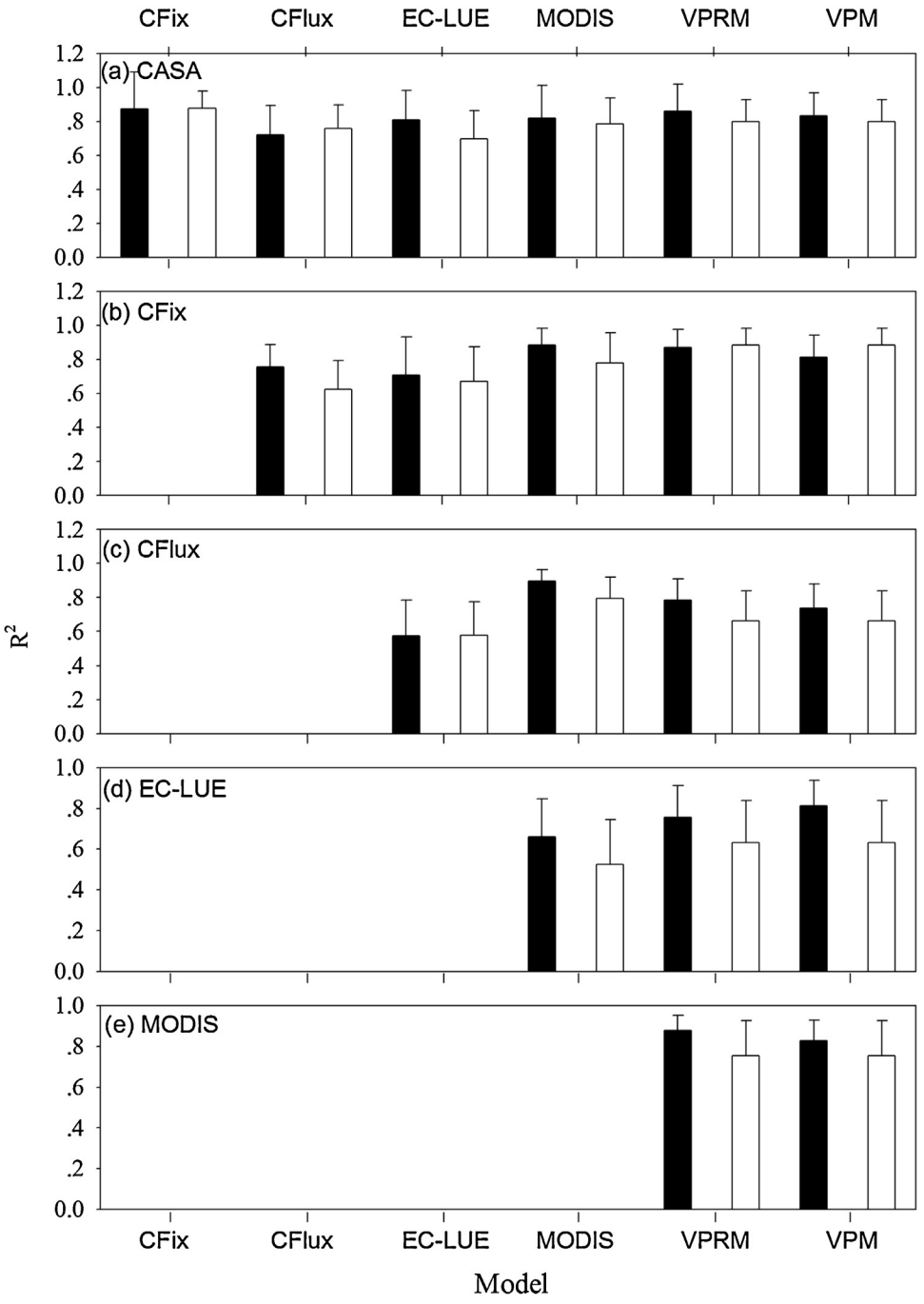

Fig. 8. Comparison of coefficient of determination (R^2) of actual light energy use only considering temperature stress (GPP_{tem}, black bars) and water stress (GPP_{water}, white bars) among LUE modes.

Table 2
Comparison of water stress levels calculated by seven LUE models.

	CASA	CFix	CFlux	EC-LUE	MODIS	VPRM/VPM[a]
CASA	–	38 ± 12%	15 ± 28%	49 ± 12%	57 ± 15%	56 ± 13%
CFix		–	43 ± 12%	42 ± 10%	53 ± 16%	46 ± 18%
CFlux	12 ± 5%	11 ± 4%	–	6 ± 6%	50 ± 15%	54 ± 12%
EC-LUE	9 ± 4%	10 ± 3%	52 ± 12%	–	65 ± 11%	58 ± 11%
MODIS	16 ± 9%	15 ± 7%	18 ± 9%	19 ± 9%	–	61 ± 12%
VPRM/VPM	16 ± 10%	12 ± 3%	13 ± 9%	22 ± 14%	17 ± 10%	–

[a] VPM and VPRM models use the same water stress equation. The values above the matrix diagonal are inconsistent percentages of identifying low, normal and high water stress conditions between two models, while the values below the matrix diagonal indicate inconsistent percentages of identifying low and high water stress conditions (please see Section 2).

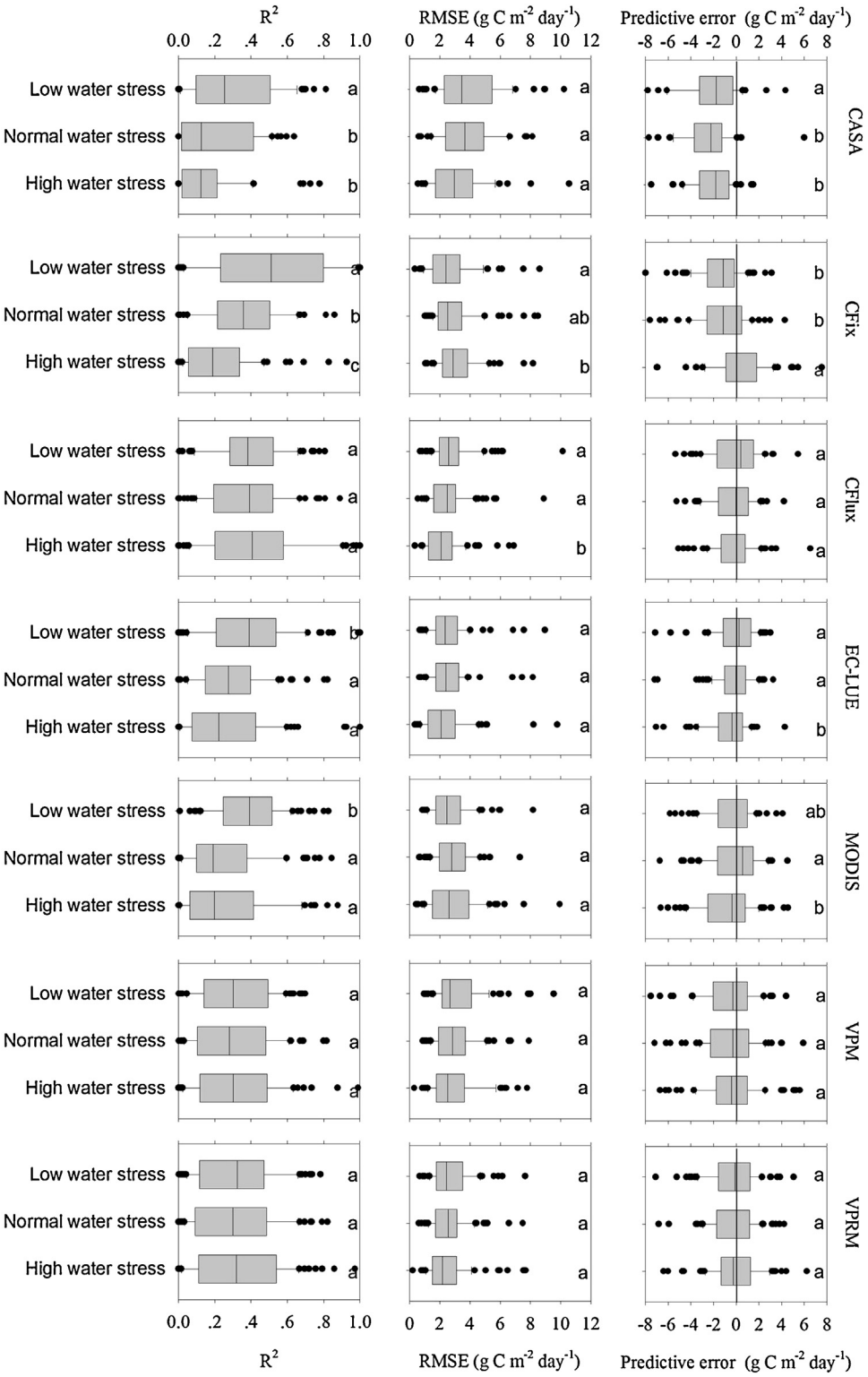

Fig. 9. The model performance for high, normal and low water stresses for seven models. Different letters within the figures indicate statistically significant differences ($p < 0.05$).

satellite data would induce inaccuracies in GPP simulations; and (3) current water downward regulation equations do not characterize the impact of water stress on GPP.

4.2. Capacity to reproduce GPP in cloudy days

Model performance depends strongly on model algorithms, and the major processes and the response of GPP to changing environmental conditions. In this study the LUE models did not seem to adequately capture the environmental regulation on vegetation production. Most LUE models only parameterize the impacts of temperature and water while only a few consider the impacts of stand age and CO_2 fertilization on vegetation production, despite the fact that previous studies have shown significant regulation of production from those factors (White et al., 1999; DeLucia and Thomas, 2000; Law et al., 2001). Our results suggest that most

models underestimated the GPP on cloudy days, likely because they do not parameterize the impacts of diffuse radiation on vegetation photosynthesis.

Previous studies have found that increased fraction of diffuse radiation during cloudy days enhanced plant photosynthesis (Law et al., 2002; Gu et al., 2002; Urban et al., 2007; Alton et al., 2007; Kasturi et al., 2012). Gu et al. (2003) reported increases in diffuse radiation caused by volcanic aerosols enhanced midday photosynthesis of a deciduous forest by 23% in 1992 and 8% in 1993. This finding contributed to the temporary increase of terrestrial ecosystems carbon sink after the eruption of Mount Pinatubo (15.1° N, 121.4° E) (Ciais et al., 1995; Bousquet et al., 2000; Battle et al., 2000). Besides volcanic eruptions, clouds also reduce the global solar radiation while increasing the relative proportion of diffuse radiation at the Earth surface.

It appears that an increased fraction of diffuse radiation can be the cause of changes in many atmospheric factors such as temperature, moisture, and latent heat. These variables have direct or indirect influences on terrestrial ecosystem carbon dynamics (Gu et al., 1999). However, several other direct impacts of diffuse radiation have been found: (1) an increase of the blue/red light ratio may lead to higher photosynthesis rates per unit leaf area with increasing faction of diffuse radiation (Gu et al., 2002; Alton et al., 2007); (2) diffuse radiation penetrates to lower depths of the canopy more efficiently than direct radiation and therefore increasing the potential leaf area available for photosynthesis (Matsuda et al., 2004).

Among the seven LUE models, the CFlux is the only model that integrates the impacts of diffuse radiation on plant photosynthesis (Turner et al., 2006). The CFlux model assumes a maximum potential LUE for fully cloudy conditions and minimum values for clear days. It further includes a linear increased trend in potential LUE with larger cloud cover (Turner et al., 2006). Results of this study showed that the simple linear equation can effectively represent the impacts of diffuse radiation. He et al. (2013) developed a two-leaf LUE model based on the MOD17 algorithm, which separates the canopy into sunlit and shaded leaf groups and calculates GPP separately for them with different maximum LUEs. Although the newly developed model shows lower sensitivity to sky conditions than the MOD17 algorithm, it needs to be validated across different water geographical regions and ecosystem types. In sum, it is clear that explicitly parameterizing the effect of diffuse radiation for GPP estimation in the future is needed in order to adequately assess the role of the terrestrial ecosystems in the global carbon cycle.

4.3. Impacts of fPAR on model performance

The LUE-type model is predominantly applied in satellite-based models, where the fraction of solar radiation intercepted by terrestrial vegetation (*fPAR*) is calculated from remote sensing data. Any errors in satellite data will propagate into GPP estimations. A recent study revealed large uncertainties in the fraction in the input data of solar radiation intercepted by vegetation, which would subsequently produce the highest uncertainty in annual GPP compared with meteorology inputs (Sjöström et al., 2013).

Vegetation indices are closely related to vegetation growth conditions and have been widely used in LUE models for calculating *fPAR*. Although EVI and NDVI are complementary vegetation indices (Huete et al., 2002), there was a remarkable difference between EVI and NDVI seasonal patterns at seasonally moist tropical forest and temperate forests (Xiao et al., 2004a,b). Xiao et al. (2004a) compared the correlations between two vegetation indices (EVI, NDVI) and GPP at an evergreen needleleaf forest, and found the seasonal dynamics of EVI followed those of GPP better than NDVI in terms of phase and amplitude of GPP. In contrast, NDVI was also found to be the best index to indicate *fPAR* in subalpine grassland (Rossini et al., 2012). In our study, no significant differences in the correlation of *fPAR* and GPP were found among LUE models (data not shown).

Ruimy et al. (1994) underscored the fact that the linear relationship between *fPAR* and NDVI is an approximation, and it is only valid during the growing stage. A significant decrease in the sensitivity of NDVI was observed when *fPAR* exceeds 0.7 (Walter-Shea et al., 1997; Viña and Gitelson, 2005). The non-linear relation between NDVI and *fPAR* reported in several studies has a physical basis as described in Myneni et al. (1995) and Knyazikhin et al. (1998). Therefore one of the main problems of the remote assessment of GPP based on remote sensing data is caused by the uncertainty of the NDVI/fPAR relationship, which is normally assumed to be linear (Running et al., 2004).

MODIS fPAR product was used as input within several of the LUE models (i.e., MODIS-GPP and CFlux). However, it is possible that some contamination remains, particularly at high latitudes in which low solar angles, persistent cloud cover, and extended periods of darkness can affect reflectance readings from the optical MODIS sensor (Myneni et al., 2002). This signal contamination could affect GPP in undetermined ways. Moreover, a previous study found consistent overestimation of GPP in the spring over North America, and which suggests that there is a problem with early season estimation of *fPAR* (Heinsch et al., 2006). Another study found MODIS *fPAR* was in general higher than the in situ calculated *fPAR* of dry periods at center Africa grassland, and failed to capture the green-up (Sjöström et al., 2013).

4.4. Impacts of water stress on model performance

Differences in model structure have been considered as the most important sources of variation among models simulations. In this study, we conducted two pairwise comparisons, and found different parameterizations of water stress dominated the sources of model differences. Defining a function used by remote sensing to capture the constraint of moisture availability on plant photosynthesis has already been a challenge for many years. The effects of water availability on GPP have been estimated in different ways in various LUE models, including as a function of soil moisture, evaporative fraction and atmospheric vapor pressure deficit (Field et al., 1995; Prince and Goward, 1995). As one example, in the EC-LUE model, water stress is estimated using the ratio of actual evapotranspiration to net shortwave radiation since decreasing amounts of energy partitioned to evaporate water suggests a stronger moisture limitation (Kurc and Small, 2004; Zhang et al., 2004; Suleiman and Crago, 2004; Chen et al., 2014). Other models, such as the VPM and VPRM, use a satellite-derived water index (Land Surface Water Index) to estimate the seasonal dynamics of water stress (Xiao et al., 2004a).

It remains difficult to characterize water available for plants and its effect on photosynthesis over large areas from either modeling or remote sensing and this limits the accuracy of any spatial GPP model. All water-related variables used in LUE models have several advantages/disadvantages in terms of representing the constraint of water availability, whilst being practical to implement. Previous studies indicated vapor pressure deficit is not a good indicator of the spatial heterogeneity of soil moisture conditions across the landscape (e.g., slope versus valley) and it is not likely to be linearly related to soil water availability for which it is often used as a proxy (Yuan et al., 2007a). Moreover, the evaporative fraction needs an ET model for simulating ecosystem evapotranspiration which will further reduce the LUE model performance (Mu et al., 2013). For satellite-derived water index (e.g., Land Surface Water Index), a previous study reported different sensitivity to soil and vegetation liquid water content, and especially its performance is weak in the high rainfall regions (Chandrasekar et al., 2010).

On the other hand, LUE models highlight the practicality of estimating GPP, and models excluded many physiological processes in the model algorithms. It has been suggested that plants have evolved comprehensive adaptive mechanisms for maintaining high photosynthesis even during the dry periods. For example, large areas of savannas are able to access the soil moisture to persist through the dry season despite extremely low soil moisture contents which means that atmospheric and surface moisture deficit may be decoupled from photosynthesis (Yuan et al., 2007b; Beringer et al., 2011). Numerous studies have revealed climate induced physiological responses are greater than the direct effect of climatic variability on the carbon cycle (Braswell et al., 1997; Hui et al., 2003; Richardson et al., 2007; Yuan et al., 2009). For example, at seasonally moist tropical evergreen forests, plants reproduce deep root system for access to water in deep soils and are able to mitigate water stress (Nepstad et al., 1994). Therefore, information on plant physiological adaptive mechanisms is critically needed for GPP models in order to accurately simulate the impacts of water stress.

5. Summary

We evaluated seven satellite-driven light use efficiency models against 157 eddy covariance sites globally covering major ecosystem types. All seven models showed the best model performance at deciduous broadleaf forests and mixed forests, intermediate performance at grasslands and evergreen needleleaf forests, and the worst at evergreen broadleaf forests and shrublands. Spatially, the CFlux and EC-LUE showed higher correlations between site-averaged GPP derived from eddy covariance towers and simulated GPP, and showed a better performance to simulate interannual variability of GPP than other models. The *fPAR*, temperature and water stress equations differed greatly among the seven LUE models. Water stress algorithms generated the largest variation between models compared to temperature factors. This study suggests that there is a need to integrate more detailed ecophysiological knowledge, especially considering the impacts of diffuse radiation on light use efficiency, and develop reliable water limitation equations in order to improve the abilities of LUE models.

Acknowledgments

This study was supported by the National Science Foundation for Excellent Young Scholars of China (41322005), the National High Technology Research and Development Program of China (863 Program) (2013AA122003, 2013AA122800), Program for New Century Excellent Talents in University (NCET-12-0060), LCLUC Program of NASA, Innovation Teams Program of Hunan Natural Science Foundation of China (2013 #7), and IceMe of the NUIST. This work used eddy covariance data acquired by the FLUXNET community and in particular by the following networks: AmeriFlux (U.S. Department of Energy, Biological and Environmental Research, Terrestrial Carbon Program (DE-FG02-04ER63917 and DE-FG02-04ER63911)), AfriFlux, AsiaFlux, CarboAfrica, CarboEuropeIP, CarboItaly, CarboMont, ChinaFlux, Fluxnet-Canada (supported by CFCAS, NSERC, BIOCAP, Environment Canada, and NRCan), GreenGrass, KoFlux, LBA, NECC, OzFlux, TCOS-Siberia, and the USCCC. We acknowledge the financial support to the eddy covariance data harmonization provided by GHG-Europe, FAO-GTOS-TCO, iLEAPS, Max Planck Institute for Biogeochemistry, National Science Foundation, University of Tuscia, Université Laval, Environment Canada and US Department of Energy and the database development and technical support from Berkeley Water Center, Lawrence Berkeley National Laboratory, Microsoft Research eScience, Oak Ridge National Laboratory, University of California – Berkeley and the University of Virginia.

Appendix A. Supplementary data

Supplementary data associated with this article can be found, in the online version, at http://dx.doi.org/10.1016/j.agrformet.2014.03.007.

References

Alton, P.B., North, P.R., Los, S.O., 2007. The impact of diffuse sunlight on canopy light-use efficiency, gross photosynthetic product and net ecosystem exchange in three forest biomes. Global Change Biol. 143, 776–787.

Battle, M., Bender, M.L., Tans, P.P., White, J.W.C., Ellis, J.T., Conway, T., Francey, R.J., 2000. Global carbon sinks and their variability inferred from atmospheric O_2 and $\delta^{13}C$. Science 287, 2467–2470.

Bunn, A.G., Goetz, S.J., 2006. Trends in satellite-observed circumpolar photosynthetic activity from 1982 to 2003: the influence of seasonality, cover type, and vegetation density. Earth Interact. 1012, 1–19.

Beringer, J., Hacker, J., Hutley, L.B., Leuning, R., Arndt, S.K., Amiri, R., Bannehr, L., Cernusak, L.A., Grover, S., Hensley, C., Hocking, D., Isaac, P., Jamali, H., Kanniah, K., Livesley, S., Neininger, B., Paw, U.K.T., Sea, W., Straten, D., Tapper, N., Weinmann, R., Wood, S., Zegelin, S., 2011. SPECIAL-savanna patterns of energy and carbon integrated across the landscape. Bull. Am. Meteorol. Soc. 92, 1467–1485.

Bousquet, P., Peylin, P., Ciais, P., Le Quéré, C., Friedlingstein, P., Tans, P.P., 2000. Regional changes in carbon dioxide fluxes of land and ocean since 1980. Science 290, 1342–1345.

Beer, C., Reichstein, M., Tomelleri, E., Ciais, P., Jung, M., Carvalhais, N., Rödenbeck, C., Arain, M.A., Baldocchi, D., Bonan, G.B., Bondeau, A., Cescatti, A., Lasslop, G., Lindroth, A., Lomas, M., Luyssaert, S., Margolis, H., Oleson, K.W., Roupsard, O., Veenendaal, E., Viovy, N., Williams, C., Woodward, F.I., Papale, D., 2010. Terrestrial gross carbon dioxide uptake: global distribution and covariation with climate. Science 329, 834–838.

Braswell, B.H., Schimel, D.S., Linder, E., Moore, B., 1997. The response of global terrestrial ecosystems to interannual temperature variability. Science 278, 870–872.

Cai, W.W., Yuan, W.P., Liang, S.L., Zhang, X.T., Dong, W.J., Xia, J.Z., Fu, Y., Chen, Y., Liu, D., Zhang, Q., 2014. Improved estimations of gross primary production using satellite-derived photosynthetically active radiation. J. Geophys. Res.: Biosci. 119, http://dx.doi.org/10.1002/2013JG002456.

Chen, Y., Xia, J.Z., Liang, S.L., Feng, J.M., Fisher, J.B., Li, X., Li, X.L., Liu, S.G., Ma, Z.G., Miyata, A., Mu, Q.Z., Sun, L., Tang, J.W., Wang, K.C., Wen, J., Xue, Y.J., Yu, G.R., Zha, T.G., Zhang, L., Zhang, Q., Zhoa, T.B., Zhao, L., Yuan, W.P., 2014. Comparison of evapotranspiration models over terrestrial ecosystem in China. Remote Sens. Environ. 140, 279–293.

Cramer, W., Kicklighter, D.W., Bondeau, A., Moore, B., Churkina, C., Nemry, B., Ruimy, A., 1999. Comparing global models of terrestrial net primary productivity NPP: overview and key results. Global Change Biol. 5, 1–15.

Canadell, J.G., Kirschbaum, M.U.F., Kurz, W.A., Sanz, M.-J., Schlamadinger, B., Yamagata, Y., 2007. Factoring out natural and indirect human effects on terrestrial carbon sources and sinks. Environ. Sci. Pol. 104, 370–384.

Chandrasekar, K., Sesha Sai, M.V.R., Roy, P.S., Dwevedi, R.S., 2010. Land surface water index response to rainfall and NDVI using the MODIS vegetation index product. Int. J. Remote Sens. 31, 3987–4005.

Ciais, P., Tans, P.P., Trolier, M., White, J.W.C., Francey, R.J., 1995. A large northern hemisphere terrestrial CO_2 sink indicated by the $^{13}C/^{12}C$ ratio of atmospheric CO_2. Science 269, 1098–1102.

Coops, N.C., Waring, R.H., Law, B.E., 2005. Assessing the past and future distribution and productivity of ponderosa pine in the Pacific Northwest using a process model, 3-PG. Ecol. Modell. 1831, 107–124.

DeLucia, E., Thomas, R., 2000. Photosynthetic responses to CO_2 enrichment of four hardwood species in a forest understory. Oecologia 1221, 11–19.

Field, C.B., Jackson, R.B., Mooney, H.A., 1995. Stomatal responses to increased CO_2: implications from the plant to the global scale. Plant. Cell Environ. 1810, 1214–1225.

Gu, L., Baldocchi, D., Verma, S.B., Black, T.A., Vesala, T., Falge, E.M., Dowty, P.R., 2002. Advantages of diffuse radiation for terrestrial ecosystem productivity. J. Geophys. Res.: Atmos. 107, ACL 2-1–ACL 2-23.

Gu, L.H., Baldocchi, D., Wofsy, S.C., Munger, J.W., Michalsky, J.J., Urbanski, S.P., Boden, T.A., 2003. Response of a deciduous forest to the Mount Pinatubo eruption: enhanced photosynthesis. Science 299, 2035–2038.

Gu, L.H., Fuentes, J.D., Shugart, H.H., Staebler, R.M., Black, T.A., 1999. Responses of net ecosystem exchanges of carbon dioxide to changes in cloudiness: results from two North American deciduous forests. J. Geophys. Res.: Atmos. 104, 31421–31434.

Huete, A., Didan, K., Miura, T., Rodriguez, E.P., Gao, X., Ferreira, L.G., 2002. Overview of the radiometric and biophysical performance of the MODIS vegetation indices. Remote Sens. Environ. 83, 195–213.

He, M.Z., Ju, W.M., Zhou, Y.L., Chen, J.M., He, H.L., Wang, S.Q., Wang, H.M., Guan, D.X., Yan, J.H., Li, Y.N., Hao, Y.B., Zhao, F.H., 2013. Development of a two-leaf light use efficiency model for improving the calculation of terrestrial gross primary productivity. Agric. Forest Meteorol. 173, 28–39.

Hui, D., Luo, Y., Katul, G., 2003. Partitioning interannual variability in net ecosystem exchange between climatic variability and functional change. Tree Physiol. 237, 433–442.

Huntzinger, D.N., Post, W.M., Wei, Y., Michalak, A.M., West, T.O., Jacobson, A.R., Baker, I.T., Chen, J.M., Davis, K.J., Hayes, D.J., Hoffman, F.M., Jain, A.K., Liu, S., McGuire, A.D., Neilson, R.P., Potter, C., Poulter, B., Price, D., Raczka, B.M., Tian, H.Q., Thornton, P., Tomelleri, E., Viovy, N., Xiao, J., Yuan, W., Zeng, N., Zhao, M., Cook, R., 2012. North American Carbon Program NACP regional interim synthesis: terrestrial biospheric model intercomparison. Ecol. Modell. 232, 144–157.

Heinsch, F.A., Zhao, M., Running, S.W., Kimball, J.S., Nemani, R.R., Davis, K.J., Bolstad, P.V., Cook, B.D., Desai, A.R., Ricciuto, D.M., Law, B.E., Oechel, W.C., Kwon, H., Luo, H., Wofsy, S.C., Dunn, A.L., Munger, J.W., Baldocchi, D.D., Xu, L., Hollinger, D.Y., Richardson, A.D., Stoy, P.C., Siqueira, M.B.S., Monson, R.K., Burns, S.P., Flanagan, L.B., 2006. Evaluation of remote sensing based terrestrial productivity from MODIS using regional tower eddy flux network observations. IEEE Trans. Geosci. Remote Sens. 447, 1908–1925.

Keenan, T.F., Baker, I., Barr, A., Ciais, P., Davis, K., Dietze, M., Dragoni, D., Gough, C.M., Grant, R., Hollinger, D., Hufkens, K., Poulter, B., McCaughey, H., Raczka, B., Ryu, Y., Schaefer, K., Tian, H., Verbeeck, H., Zhao, M., Richardson, A.D., 2012. Terrestrial biosphere model performance for inter-annual variability of land-atmosphere CO_2 exchange. Global Change Biol. 186, 1971–1987.

Kasturi, K.D., Beringer, J., North, P., Hutley, L., 2012. Control of atmospheric particles on diffuse radiation and terrestrial plant productivity: a review. Progr. Phys. Geogr. 36, 209–237.

Knyazikhin, Y., Martonchik, J.V., Myneni, R.B., Diner, D.J., Running, S.W., 1998. Synergistic algorithm for estimating vegetation canopy leaf area index and fraction of absorbed photosynthetically active radiation from MODIS and MISR data. J. Geophys. Res.: Biogeosci. 103, 32257–32274.

Kurc, S.A., Small, E.E., 2004. Dynamics of evapotranspiration in semiarid grassland and shrubland ecosystems during the summer monsoon season, central New Mexico. Water Resour. Res. 40, W09305.

King, D.A., Turner, D.P., Ritts, W.D., 2011. Parameterization of a diagnostic carbon cycle model for continental scale application. Remote Sens. Environ. 1157, 1653–1664.

Landsberg, J.J., 1986. Physiological Ecology of Forest Production. Academic Press, London, pp. 165–178.

Law, B.E., Falge, E., Baldocchi, D.D., Bakwin, P., Berbigier, P., Davis, K., Dolman, A.J., Falk, M., Fuentes, J.D., Goldstein, A., Granier, A., Grelle, A., Hollinger, D., Janssens, I.A., Jarvis, P., Jensen, N.O., Katul, G., Mahli, Y., Matteucci, G., Monson, R., Munger, W., Oechel, W., Olson, R., Pilegaard, K., Paw, U.K.T., Thorgeirsson, H., Valentini, R., Verma, S., Vesala, T., Wilson, K., Wofsy, S., 2002. Environmental controls over carbon dioxide and water vapor exchange of terrestrial vegetation. Agric. Forest Meteorol. 113, 97–120.

Law, B.E., Thornton, P., Irvine, J., Anthoni, P., Tuyl, S.V., 2001. Carbon storage and fluxes in ponderosa pine forests at different developmental stages. Global Change Biol. 7, 755–777.

Landsberg, J.J., Waring, R.H., 1997. A generalised model of forest productivity using simplified concepts of radiation-use efficiency, carbon balance and partitioning. Forest Ecol. Manage. 953, 209–228.

Law, B.E., Waring, R.H., Anthoni, P.M., Aber, J.D., 2000. Measurements of gross and net ecosystem productivity and water vapor exchange of a *Pinus ponderosa* ecosystem, and an evaluation of two generalized models. Global Change Biol. 6, 155–168.

Li, X.L., Liang, S.L., Yu, G.R., Yuan, W.P., Cheng, X., Xia, J.Z., Zhao, T.B., Feng, J.M., Ma, Z.G., Ma, M.G., Liu, S.M., Chen, J.Q., Shao, C.L., Li, S.G., Zhang, X.D., Zhang, Z.Q., Chen, S.P., Ohta, T., Varlagin, A., Miyata, A., Takagi, K., Saiqusa, N., Kato, T., 2013. Estimation of gross primary production over the terrestrial ecosystems in China. Ecol. Modell., 80–92, 261–262.

Lloyd, J., Taylor, J.A., 1994. On the Temperature Dependence of Soil Respiration. Functional Ecology 8, 315–323.

Myneni, R.B., Hoffman, S., Knyazikhin, Y., Privette, J.L., Glassy, J., Tian, Y., Wang, Y., Song, X., Zhang, Y., Smith, G.R., Lotsch, A., Friedl, M., Morisette, J.T., Votava, P., Nemani, R.R., Running, S.W., 2002. Global products of vegetation leaf area and fraction absorbed PAR from year one of MODIS data. Remote Sens. Environ. 83, 214–231.

Myneni, R.B., Hall, F.G., Sellers, P.J., Marshak, A.L., 1995. The meaning of spectral vegetation indices. IEEE Trans. Geosci. Remote Sens. 33, 481–486.

Matsuda, R., Ohashi-Kaneko, K., Fujiwara, K., Goto, E., Kurata, K., 2004. Photosynthetic characteristics of rice leaves grown under red light with or without supplemental blue light. Plant Cell Physiol. 4512, 1870–1874.

Mahadevan, P., Wofsy, S.C., Matross, D.M., Xiao, X.M., Dunn, A.L., Lin, J.C., Gerbig, C., Munger, J.W., Chow, V.Y., Gottlieb, E.W., 2008. A satellite-based biosphere parameterization for net ecosystem CO_2 exchange: Vegetation Photosynthesis and Respiration Model VPRM. Global Biogeochem. Cycles 222, 1–17.

Mu, Q., Zhao, M., Kimball, J.S., McDowell, N.G., Running, S.W., 2013. A remotely sensed global terrestrial drought severity index. Bull. Am. Meteorol. Soc. 94, 83–98.

Nepstad, D.C., de Carvalho, C.R., Davidson, E.A., Jipp, P.H., Lefebvre, P.A., Negreiros, G.H., da Silva, E.D., Stone, T.A., Trumbore, S.E., Vieira, S., 1994. The role of deep roots in the hydrological and carbon cycles of Amazonian forests and pastures. Nature 372, 666–669.

Prince, S.D., Goward, S.N., 1995. Global primary production: a remote sensing approach. J. Biogeogr. 22, 815–835.

Potter, C.S., Randerson, J.T., Field, C.B., Matson, P.A., Vitousek, P.M., Mooney, H.A., Klooster, S.A., 1993. Terrestrial ecosystem production: a process model based on global satellite and surface data. Global Biogeochem. Cycles 74, 811–841.

Raczka, B.M., Davis, K.J., Huntzinger, D.N., Neilson, R., Poulter, B., Richardson, A., Xiao, J.F., Baker, I., Ciais, P., Keenan, T.F., Law, B., Post, W.M., Ricciuto, D., Schaefer, K., Tian, H.Q., Tomelleri, E., Verbeeck, H., Viovy, N., 2013. Evaluation of continental carbon cycle simulations with North American flux tower observations. Ecol. Monogr., http://dx.doi.org/10.1890/12-0893.1.

Reichstein, M., Falge, E., Baldocchi, D., Papale, D., Valentini, R., Aubinet, M., Berbigier, P., Bernhofer, C., Buchmann, N., Gilmanov, T., Granier, A., Grünwald, T., Havránková, K., Janous, D., Knohl, A., Laurela, T., Lohila, A., Loustau, D., Matteucci, G., Meyers, T., Miglietta, F., Ourcival, J.-M., Rambal, S., Rotenberg, E., Sanz, M., Seufert, G., Vaccari, F., Vesala, T., Yakir, D., 2005. On the separation of net ecosystem exchange into assimilation and ecosystem respiration: review and improved algorithm. Global Change Biol. 11, 1424–1439.

Rossini, M., Cogliati, S., Meroni, M., Migliavacca, M., Galvagno, M., Busetto, L., Cremonese, E., Julitta, T., Siniscalco, C., di Cella, M.U., Colombo, R., 2012. Remote sensing-based estimation of gross primary production in a subalpine grassland. Biogeosciences 97, 2565–2584.

Richardson, A., Hollinger, D., Aber, J., Ollinger, S., Braswell, B., 2007. Environmental variation is directly responsible for short but not long term variation in forest atmosphere carbon exchange. Global Change Biol. 13, 788–803.

Running, S.W., Nemani, R.R., Heinsch, F.A., Zhao, M., Reeves, M., Hashimoto, H., 2004. A continuous satellite-derived measure of global terrestrial primary production. Biosciences 546, 547–560.

Ruimy, A., Saugier, B., Dedieu, G., 1994. Methodology for the estimation of terrestrial net primary production from remotely sensed data. J. Geophys. Res.: Atmos. 99, 5263–5283.

Schimel, D., 2007. Carbon cycle conundrums. Proc. Natl. Acad. Sci. USA 10447, 18353–18354.

Suleiman, A., Crago, R., 2004. Hourly and daytime evapotranspiration from grassland using radiometric surface temperatures. Agron. J. 96, 384–390.

Sjöström, M., Zhao, M., Archibal, S., Arneth, A., Cappelaere, B., Falk, U., de Grandcourt, A., Hanan, N., Kergoat, L., Kutsch, W., Merbold, L., Mougin, E., Nickless, A., Nouvellon, Y., Scholes, R.J., Veenendaal, E.M., Ardö, J., 2013. Evaluation of MODIS gross primary productivity for Africa using eddy covariance data. Remote Sens. Environ. 131, 275–286.

Turner, D.P., Ritts, W.D., Styles, J.M., Yang, Z., Cohen, W.B., Law, B.E., Thornton, P.E., 2006. A diagnostic carbon flux model to monitor the effects of disturbance and interannual variation in climate on regional NEP. Tellus B. 585, 476–490.

Urban, O., Janouš, D., Acosta, M., Czerný, R., Marková, I., Navrátil, M., Pavelka, M., Pokorný, R., Šprtová, M., Zhang, R., Špunda, V., Grace, J., Marek, M.V., 2007. Ecophysiological controls over the net ecosystem exchange of mountain spruce stand: comparison of the response in direct vs. diffuse solar radiation. Global Change Biol. 131, 157–168.

Viña, A., Gitelson, A.A., 2005. New developments in the remote estimation of the fraction of absorbed photosynthetically active radiationin crops. Geophys. Res. Lett. 32, L17403.

Veroustraete, F., Sabbe, H., Eerens, H., 2002. Estimation of carbon mass fluxes over Europe using the C-Fix model and Euroflux data. Remote Sens. Environ. 833, 376–399.

Walter-Shea, E.A., Privette, J., Cornell, D., Mesarch, M.A., Hays, C.J., 1997. Relations between directional spectral vegetation indices and leaf area and absorbed radiation in alfalfa. Remote Sens. Environ. 611, 162–177.

White, M.A., Running, S.W., Thornton, P.E., 1999. The impact of growing-season length variability on carbon assimilation and evapotranspiration over 88 years in the eastern US deciduous forest. Int. J. Biometeorol. 423, 139–145.

Xiao, X., Hollinger, D., Aber, J., Goltzc, M., Davidson, E.A., Zhang, Q., Moore III, B., 2004a. Satellite-based modeling of gross primary production in an evergreen needleleaf forest. Remote Sens. Environ. 89, 519–534.

Xiao, X.M., Zhang, Q.Y., Braswell, B., Urbanski, S., Boles, S., Wofsy, S., Moore III, B., Ojim, D., 2004b. Modeling gross primary production of temperate deciduous broadleaf forest using satellite images and climate data. Remote Sens. Environ. 912, 256–270.

Yuan, W.P., Luo, Y.Q., Richardson, A.D., Oren, R., Luzssaert, S., Janssens, J.A., Ceulemans, R., Zhou, X., Grünwald, T., Aubinet, M., Berhofer, C., Baldocchi, D.D., Chen, J.Q., Dunn, A.L., Deforest, J.L., Dragon, D., Goldstein, A.H., Moors, E., Munger, J.M., Monson, R.K., Suzker, A.E., Starr, G., Scott, R.L., Tenhunen, J., Verma, S.H., Vesala, T., Wofsy, S.C., 2009. Latitudinal patterns of magnitude and interannual variability in net ecosystem exchange regulated by biological and environmental variables. Global Change Biol. 15, 2905–2920.

Yuan, W.P., Liu, S.G., Yu, G.R., Bonnefond, J.M., Chen, J.Q., Davis, K., Desai, A.R., Goldstein, A.H., Gianelle, D., Rossi, F., Suyker, A.E., Verma, S.B., 2010. Global estimates of evapotranspiration and gross primary production based on MODIS and global meteorology data. Remote Sens. Environ. 1147, 1416–1431.

Yuan, W.P., Liu, S.G., Zhou, G.S., Zhou, G.Y., Tieszen, L.L., Baldocchi, D., Bernhofer, C., Gholz, H., Goldstein, A.H., Goulden, M.L., Hollinger, D.Y., Hu, Y., Lawn, B.E., Stoy, P.C., Vesala, T., Wofsy, S.C., 2007a. Deriving a light use efficiency model from eddy covariance flux data for predicting daily gross primary production across biomes. Agric. Forest Meteorol. 1433, 189–207.

Yuan, W.P., Zhou, G.S., Wang, Y.H., Han, X., Wang, Y.S., 2007b. Simulating phenological characteristics of two dominant grass species in a semi-arid steppe ecosystem. Ecol. Res. 22, 784–791.

Yuan, W.P., Liang, S.L., Liu, S.G., Weng, E.S., Luo, Y.Q., Hollinger, D., Zhang, H.C., 2012. Improving model parameter estimation using coupling relationships between vegetation production and ecosystem respiration. Ecol. Modell. 240, 29–40.

Zhang, Y.Q., Liu, C.M., Yu, Q., Shen, Y.J., Kendy, E., Kondoh, A., Tang, C., Sun, H., 2004. Energy fluxes and the Priestley–Taylor parameter over winter wheat and maize in the North China Plain. Hydrol. Process. 1812, 2235–2246.